Available online at www.sciencedirect.com

ScienceDirect

Procedia Technology 14 (2014) 133 – 140

Procedia Technology

2nd International Conference on Innovations in Automation and Mechatronics Engineering, ICIAME 2014

# Optimized Configurations of Kinematically Redundant Planar Parallel Manipulator following a Desired Trajectory

K V Varalakshmi[a,]* , J Srinivas[a]

[a,b]*Department of Mechannical Engg., National Institute of Technology, Rourkela, Odisha 769008, India*

**Abstract**

This paper presents an optimization methodology for achieving minimum actuation torques of a kinematically redundant planar parallel mechanism following a desired trajectory using binary coded Genetic Algorithms (GA). A user interactive computer program developed in present work helps for obtaining inverse kinematic solution and Jacobian matrices at a given Cartesian coordinate location of the end-effector. Furthermore, the joint torques are obtained from the end-effector forces (wrench) using Jacobian matrix at every location. The resultant joint torque vector can be used to describe the objective function. The variables of the optimization problem are redundant base prismatic joint displacements and the constraints include the variable bounds and the pre-defined trajectory lying within the original workspace. The outputs of the kinematically-redundant 3-PRRR manipulator are compared against the results for a non-redundant 3-RRR manipulator. The results show that the redundant manipulator gives relatively lower input torques. Also, it is observed that while passing through singular configurations on the trajectory, finite values of torques are achieved. Results are shown for a straight-line trajectory.



Peer-review under responsibility of the Organizing Committee of ICIAME 2014.

*Keywords:* Kinematic redundancy; planar parallel manipulator; staic force analysis; minimum joint torques; non-conventional optimization

**Nomenclature**

| | | | | | |
|---|---|---|---|---|---|
| **q** | joint displacements | $\boldsymbol{n}_i$ | unit vector directed along the distal links | $\rho_i$ | prismatic joint limits |
| **x** | end-effector pose | $l_{1i}$, $l_{2i}$ | link lengths of active and passive links | **R** | rotation matrix |
| $\mathbf{J_X}$ | inverse Jacobian | $\theta_i$ | active joint angles ($i$=1,2,3) | ***Z*** | unit vector along Z direction |
| **Jq** | direct Jacobian | $\beta_i$ | passive joint angles ($i$=1,2,3) | ***F*** | force vector |

* Corresponding author. Tel.: +918763989679;
*E-mail address:* kv.varalakshmi@gmail.com



Peer-review under responsibility of the Organizing Committee of ICIAME 2014.
doi:10.1016/j.protcy.2014.08.018

| | | | | | |
|---|---|---|---|---|---|
| **OP** | vector expressing point P | $\alpha_i$ | prismatic joint angles ($i$=1,2,3) | $\boldsymbol{\tau}$ | torque |
| $f$ | objective function | $\boldsymbol{PC}'_i$ | vector from P to $C_i$ w.r.to xy | | |

## 1. Introduction

Redundancy in parallel manipulators is generally divided into kinematic redundancy and actuation redundancy here they explained in terms of mobility. When the manipulator mobility is larger than the required degrees of freedom (DOF), it is kinematic redundancy. On the other hand, when the number of actuators in the manipulator is larger than the mobility, it is actuation redundancy. However, most of the studies [1]–[2] have discussed on actuation redundancy, in this the manipulator is controlled with more actuators than the required without increasing the mobility. Recently some of the researches have been discussed on kinematic redundancy [3]–[4]. This type of redundancy can enhance the dexterity of the manipulator as well as enlarge the workspace. Additionally kinematically redundant parallel manipulators have been widely used to improve the trajectory tracking performance by effectively increasing the singularity-free region in the workspace. Wang and Gosselin [5] and Ebrahimi et al. [6]-[7] studied the singularity of three new types of kinematically redundant parallel manipulators. It was shown that the singularity free configurations are significantly improved when compared to the non-redundant manipulator. Cha et al. [8]-[9] proposed a kinematic redundancy resolution algorithm for singularity avoidance of the 3-RRR mechanism and to determine the allowable ranges of the kinematically redundant active prismatic joint variables for a given trajectory to be in singularity free region. Most of the research works focused on dealing the kinematic design, workspace and singularity avoidance, very few authors dealt force capabilities of kinematically-redundant planar parallel manipulators. Weihmann et al. [10] proposed an optimization-based method for determining the force capabilities of the 3-RPRR manipulator. Here path of the manipulator is not considered. Boudreau [11] developed an optimization-based methodology for resolving the generalized forces for kinematically-redundant planar parallel manipulator following a desired trajectory and achieved improved results compared to non-redundant manipulator.

Present work concerns with the kinematic analysis of 3-PRRR kinematically redundant mechanism of three different degrees of freedom and gives attention on the determination of joint-torques using static force analysis. A suitable end-effector trajectory is selected and the nonlinear joint torques at each trajectory point are minimized by selecting optimum locations of prismatic joints on the base links using binary coded genetic algorithms. If it is of first order redundancy, random search may resolve the problem. Optimized torques are illustrated for a trajectory passing through singular points.

## 2. Description of kinematically redundant linkages

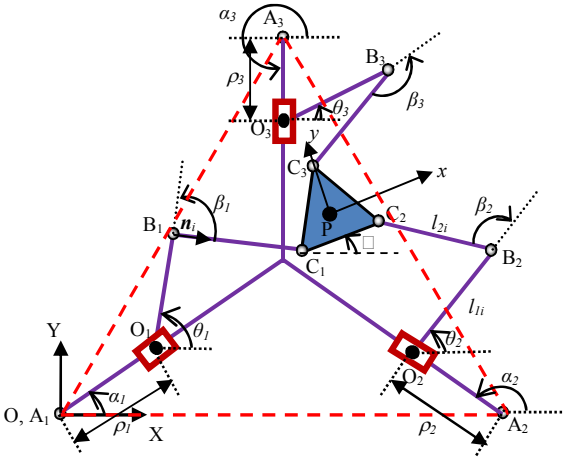


Fig. 1 Redundant 3-PRRR manipulator configuration

The redundant 3-PRRR planar parallel manipulator as shown in Fig.1 consists of a three branches, each composed of an actuated revolute joint fixed to the base, followed by passive revolute joints, one of which is attached to the moving platform (end-effector). If the points $A_i$ coincides with $O_i$ ($i$ = 1, 2, 3), then the configuration is non-redundant 3-RRR manipulator. The basic configuration of redundant 3-PRRR mechanism is derived by adding extra active prismatic joints to the limbs of the 3-RRR manipulator. The added prismatic actuators allow any arbitrary base joints. Adding one degree of kinematic redundancy (1-DOKR) can considerably reduce the number of direct kinematic singularities of a 3-RRR planar manipulator up to certain extent [5]. Hence, one degree of kinematic redundancy is added here in each case to each branch of the 3-RRR manipulator producing manipulators with 1-DOKR, 2-DOKR and 3-DOKR respectively. The added kinematic redundancies enable the manipulators to avoid kinematic singularities, improve their manoeuvrability, and enlarge their reachable and dexterous workspaces and also causes less dynamic effects due to the weight of the actuators when they are close to the base.

## 3. Jacobian formulation for 3-RRR and 3-PRRR manipulators

The velocity equation showing the Jacobian matrices of the manipulators resulting from differentiating the non-linear loop-closure equations $f(\mathbf{q}, \mathbf{x}) = 0$ of the input $\mathbf{q} = [\theta_1, \theta_2, \theta_3]^{\mathrm{T}}$ (joint displacements) and output $\mathbf{x} = [x, y, \phi]^{\mathrm{T}}$ (end-effector pose) variables, with respect to time, i.e.

$$\mathbf{J}_{\mathbf{x}}\dot{\mathbf{x}} = \mathbf{J}_{\mathbf{q}}\dot{\mathbf{q}} \tag{1}$$

Where $\mathbf{J}_{\mathbf{x}} = \partial \mathrm{f}(\mathbf{q}, \mathbf{x})/\partial \mathbf{x}$ and $\mathbf{J}_{\mathbf{q}} = \partial \mathrm{f}(\mathbf{q}, \mathrm{x})/\partial \mathbf{q}$ are $(m \times m)$ and $(m \times n)$ matrices respectively. Where $m$ is the DOFs in the Cartesian space and $n$ is the DOFs of the linkage (for non-redundant manipulator $m = n$; While, $\dot{\mathbf{x}}$ and $\dot{\mathbf{q}}$ are the end-effector and joint velocities, respectively. The overall Jacobian matrix $\mathbf{J}$ can be expressed as:

$$\mathbf{J} = -\mathbf{J}_{\mathbf{X}}^{-1}\mathbf{J}_{\mathbf{q}} \tag{2}$$

Where $\mathbf{J}_{\mathbf{X}}$ and $\mathbf{J}_{\mathbf{q}}$ are direct and inverse Jacobian matrices respectively. Based on the inverse displacement [3], considering the geometry of the non-redundant 3-RRR planar parallel manipulator in Fig.1, the loop closure equations can be written as by defining the unit vector $\boldsymbol{n}_i$ directed along the distal links. The following relation can thus be obtained for each kinematic chain:

$$l_{2i}\boldsymbol{n}_i = \mathbf{OP} + [\mathbf{R}]\boldsymbol{PC}_i' - \mathbf{AB}_i \tag{3}$$

By squaring on both sides of Eq.( 3) and applying the law of cosines

$$l_{2i}^2 = (\mathbf{OP} + [\mathbf{R}]\boldsymbol{PC}_i' - \mathbf{AB}_i)^{\mathrm{T}}(\mathbf{OP} + [\mathbf{R}]\boldsymbol{PC}_i' - \mathbf{AB}_i) \tag{4}$$

Where $[\mathbf{R}] = \begin{bmatrix} \cos\phi & -\sin\phi \\ \sin\phi & \cos\phi \end{bmatrix}$ is the rotation matrix, $\mathbf{OP}$ is the vector expressing point P and $\boldsymbol{PC}_i'$ is the vector from P to $C_i$ expressed in the moving frame xy.

Differentiating Eq. (4) with respect to time, the following Jacobian matrix can be obtained:

$$l_{2i}\boldsymbol{n}_i^{\mathrm{T}}\begin{bmatrix}\dot{x}\\ \dot{y}\end{bmatrix}+\mathbf{Z}^{\mathrm{T}}(\boldsymbol{PC}_i\times l_{2i}\boldsymbol{n}_i)\dot{\phi}+l_{2i}\boldsymbol{n}_i^{\mathrm{T}}\begin{bmatrix}l_{1i}\sin\theta_i\\ -l_{1i}\cos\theta_i\end{bmatrix}\dot{\theta}_i=0 \tag{5}$$

Where $\boldsymbol{Z}$ is the unit vector along z direction

It can be expressed in matrix form for all three legs as:

$$\begin{bmatrix}l_{21}\boldsymbol{n}_1^{\mathrm{T}} & \boldsymbol{Z}^{\mathrm{T}}(\boldsymbol{PC}_1\times l_{21}\boldsymbol{n}_1)\\ l_{22}\boldsymbol{n}_2^{\mathrm{T}} & \boldsymbol{Z}^{\mathrm{T}}(\boldsymbol{PC}_2\times l_{22}\boldsymbol{n}_2)\\ l_{23}\boldsymbol{n}_3^{\mathrm{T}} & \boldsymbol{Z}^{\mathrm{T}}(\boldsymbol{PC}_3\times l_{23}\boldsymbol{n}_3)\end{bmatrix}\begin{bmatrix}\dot{x}\\ \dot{y}\\ \dot{\phi}\end{bmatrix}+\begin{bmatrix}\lambda_1 & 0 & 0\\ 0 & \lambda_2 & 0\\ 0 & 0 & \lambda_3\end{bmatrix}\begin{bmatrix}\dot{\theta}_1\\ \dot{\theta}_2\\ \dot{\theta}_3\end{bmatrix}=0 \tag{6}$$

Where $\lambda_i = l_{1i}\, l_{2i}\, \boldsymbol{n}_i^{\mathrm{T}}(sin\theta_i - cos\theta_i)$

The above Eq. (6) is similar to Eq. (1) represents the Jacobian matrices of non-redundant 3-RRR planar parallel manipulator.
The loop closure equations of 3-PRRR can be expressed from Fig.1 as:

$$l_{2i}\boldsymbol{n}_i=\mathbf{OP}+[\mathbf{R}]\boldsymbol{PC}_i^{'}-\mathbf{OB}_i \tag{7}$$

$$l_{2i}^2=(\mathbf{OP}+[\mathbf{R}]\boldsymbol{PC}_i^{'}-\mathbf{OB}_i)^{\mathrm{T}}(\mathbf{OP}+[\mathbf{R}]\boldsymbol{PC}_i^{'}-\mathbf{OB}_i) \tag{8}$$

Differentiating Eq. (8) with respect to time, the following Jacobian matrices can be obtained:

$$l_{2i}\boldsymbol{n}_i^{\mathrm{T}}\begin{bmatrix}\dot{x}\\ \dot{y}\end{bmatrix}+\boldsymbol{Z}^{\mathrm{T}}(\boldsymbol{PC}_i\times l_{2i}\boldsymbol{n}_i)\dot{\phi}+l_{2i}\boldsymbol{n}_i^{\mathrm{T}}\begin{bmatrix}l_{1i}\sin\theta_i\\ -l_{1i}\cos\theta_i\end{bmatrix}\dot{\theta}_i-l_{2i}\boldsymbol{n}_i^{\mathrm{T}}\dot{\rho}_i\begin{bmatrix}cos\,\alpha_i\\ sin\,\alpha_i\end{bmatrix}=0 \tag{9}$$

It can be expressed in matrix form for all three legs of kinematically redundant linkages as:
1-DOKR:

$$\begin{bmatrix}l_{21}\boldsymbol{n}_1^{\mathrm{T}} & \boldsymbol{Z}^{\mathrm{T}}(\boldsymbol{PC}_1\times l_{21}\boldsymbol{n}_1)\\ l_{22}\boldsymbol{n}_2^{\mathrm{T}} & \boldsymbol{Z}^{\mathrm{T}}(\boldsymbol{PC}_2\times l_{22}\boldsymbol{n}_2)\\ l_{23}\boldsymbol{n}_3^{\mathrm{T}} & \boldsymbol{Z}^{\mathrm{T}}(\boldsymbol{PC}_3\times l_{23}\boldsymbol{n}_3)\end{bmatrix}\begin{bmatrix}\dot{x}\\ \dot{y}\\ \dot{\phi}\end{bmatrix}+\begin{bmatrix}\xi_1 & \lambda_1 & 0 & 0\\ 0 & 0 & \lambda_2 & 0\\ 0 & 0 & 0 & \lambda_3\end{bmatrix}\begin{bmatrix}\dot{\rho}_1\\ \dot{\theta}_1\\ \dot{\theta}_2\\ \dot{\theta}_3\end{bmatrix}=0 \tag{10}$$

2-DOKR:

$$\begin{bmatrix}l_{21}\boldsymbol{n}_1^{\mathrm{T}} & \boldsymbol{Z}^{\mathrm{T}}(\boldsymbol{PC}_1\times l_{21}\boldsymbol{n}_1)\\ l_{22}\boldsymbol{n}_2^{\mathrm{T}} & \boldsymbol{Z}^{\mathrm{T}}(\boldsymbol{PC}_2\times l_{22}\boldsymbol{n}_2)\\ l_{23}\boldsymbol{n}_3^{\mathrm{T}} & \boldsymbol{Z}^{\mathrm{T}}(\boldsymbol{PC}_3\times l_{23}\boldsymbol{n}_3)\end{bmatrix}\begin{bmatrix}\dot{x}\\ \dot{y}\\ \dot{\phi}\end{bmatrix}+\begin{bmatrix}\xi_1 & \lambda_1 & 0 & 0 & 0\\ 0 & 0 & \xi_2 & \lambda_2 & 0\\ 0 & 0 & 0 & 0 & \lambda_3\end{bmatrix}\begin{bmatrix}\dot{\rho}_1\\ \dot{\theta}_1\\ \dot{\rho}_2\\ \dot{\theta}_2\\ \dot{\theta}_3\end{bmatrix}=0 \tag{11}$$

3-DOKR:

$$\begin{bmatrix} l_{21}\boldsymbol{n}_1^{\mathrm{T}} & \boldsymbol{Z}^{\mathrm{T}}(\boldsymbol{PC}_1 \times l_{21}\boldsymbol{n}_1) \\ l_{22}\boldsymbol{n}_2^{\mathrm{T}} & \boldsymbol{Z}^{\mathrm{T}}(\boldsymbol{PC}_2 \times l_{22}\boldsymbol{n}_2) \\ l_{23}\boldsymbol{n}_3^{\mathrm{T}} & \boldsymbol{Z}^{\mathrm{T}}(\boldsymbol{PC}_3 \times l_{23}\boldsymbol{n}_3) \end{bmatrix} \begin{bmatrix} \dot{x} \\ \dot{y} \\ \dot{\phi} \end{bmatrix} + \begin{bmatrix} \xi_1 & \lambda_1 & 0 & 0 & 0 & 0 \\ 0 & 0 & \xi_2 & \lambda_2 & 0 & 0 \\ 0 & 0 & 0 & 0 & \xi_3 & \lambda_3 \end{bmatrix} \begin{bmatrix} \dot{\rho}_1 \\ \dot{\theta}_1 \\ \dot{\rho}_2 \\ \dot{\theta}_2 \\ \dot{\rho}_3 \\ \dot{\theta}_3 \end{bmatrix} = 0 \qquad (12)$$

Where $\xi_i = -l_{2i}\boldsymbol{n}_i^{\mathrm{T}}(cos\alpha_i + sin\alpha_i)$ ($i$=1, 2, 3).

The Eqs. (10, 11 and 12) are similar to Eq. (1) represents the Jacobian matrices of redundant 3-PRRR planar parallel manipulator. And the Jacobian matrices are dimensionally homogenized [3]. The developed equations allow in the computation of the velocities of the revolute and prismatic actuators for both the non-redundant and redundant cases when the velocity of the moving platform is known. Under static conditions the relationship between the joint forces/torques and the end-effector wrench is [12]:

$$\boldsymbol{F} = \mathbf{J}^{-\mathrm{T}}\boldsymbol{\tau} \qquad (13)$$

For a specified end-effector wrench $\boldsymbol{F}$ in Eq. (13) the generalized actuation joint torques/forces are given by:

$$\boldsymbol{\tau} = \mathbf{J}^{\mathrm{T}}\boldsymbol{F} \qquad (14)$$

**4. Optimization Procedure**

An optimization scheme can be described as the determination of the optimum kinematic positions of base prismatic joints in order to minimize the actuator torques subjected to the variable constrains. The multiplicity of solutions allows for minimization of the actuated joint torques required to sustain a wrench on the end-effector while following a trajectory.

The optimization problem is written as:

$$\text{Minimize} \quad \boldsymbol{\tau}^{\mathrm{T}}\boldsymbol{\tau} \qquad (15)$$

$$\text{Subject to:} \quad \rho_{i,\min} \le \rho \le \rho_{i,\max} \qquad (i=1, 2, 3) \qquad (16)$$

The optimization procedure is as follows, at each step of the trajectory:
Step 1: for a given pose, define the geometric parameters manipulator
Step 2: define a trajectory
Step 3: start with initial point of the trajectory
Step 4: generate random locations of the redundant prismatic joints within the bounds
Step 5: compute new co-ordinates of the fixed platform vertices
Step 6: using inverse kinematics numerically compute Jacobian at a point
Step 7: apply wrench on the end-effector and compute required torques using Eq. (14)
Step 8: minimize function $f(\rho_1, \rho_2, \rho_3) = \boldsymbol{\tau}^{\mathrm{T}}\boldsymbol{\tau}$, using a Genetic Algorithms optimization routine
Step 9: repeat the process from step 4 to step 8 until the trajectory has been completed.

Where $\rho_{i,\min}$ and $\rho_{i,\max}$ denote the lower and upper joint limits that guarantee the link- interference-free trajectories for the manipulator. As the joint torques are highly nonlinear functions of the joint variables, in present case, binary coded Genetic algorithms technique is employed for obtaining the configurations corresponding to minimum torque condition. Genetic algorithms being a stochastic global optimization tool can effectively solve such nonlinear formulation using three operators: reproduction, crossover and mutation. An initial population of feasible strings is updated for the next generation without losing good strings of the current population. Binary coded strings are employed for convenience and the minimum error tolerance is used as a termination criterion. More details of genetic algorithms can be found elsewhere [13].

## 5. Results and Discussion

The manipulator is considered to be used for pick and place; machining or welding operations following a given trajectory. Here a straight-line trajectory was used to show the effectiveness of the optimization. It passes through the singular (force unconstrained) configurations of the non-redundant manipulator and the results were obtained for both the non-redundant and redundant manipulators. The straight-line path trajectory with platform moving from the center of the workspace right towards the edge of the workspace, from (0.25m, 0.144m) to (0.48m, 0.144m) in increments of 1.0 mm is considered. The constant geometric parameters chosen for the manipulator are $A_iA_j$=0.5m and $C_iC_j$=0.2m, $l_{1i}$=$l_{2i}$=0.2m and □=0°. Fig.2 shows the straight line trajectory and the singular points within the constant orientation workspace of the non-redundant 3-RRR manipulator.

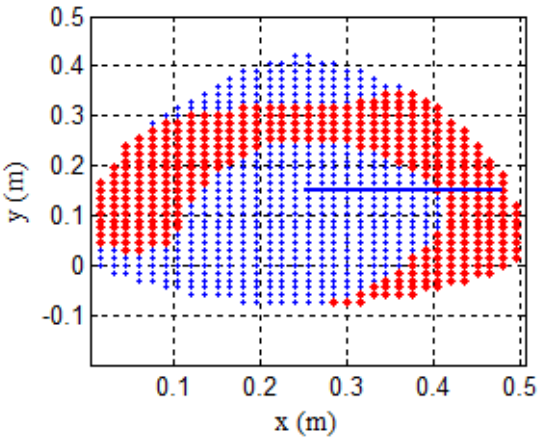


Fig. 2 Workspace and straight-line trajectory of 3-RRR linkage

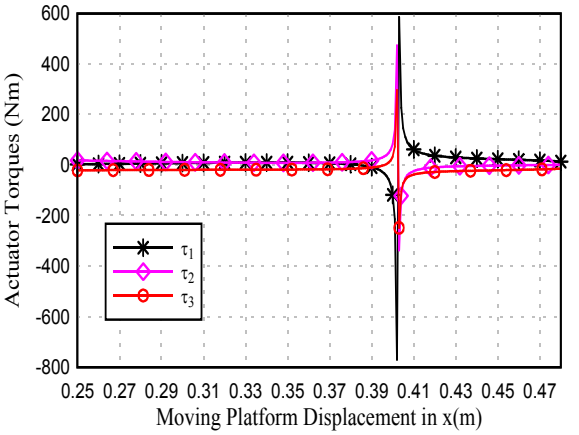


Fig. 3 Actuated torques for the 3-RRR manipulator for the Straight-line trajectory

A constant force of 46.46 N is applied on the platform in the direction opposite to the motion. Fig.3 shows the actuated torques required for the non-redundant manipulator. As can be seen from Fig.2, the manipulator passes through a singularity points from (0.405, 0.144) to (0.48, 0.144). In theory, the joint torques should reach infinity at singularity points. The finite values shown in the Fig.3 are due to the displacement step chosen, which was 1.0 mm. With a finer displacement step, the computation would have failed when the manipulator would have been exactly at the singular configuration. From the plot it is clear that the non-redundant manipulator would not be able to perform the desired trajectory, as it requires infeasible actuated torques at the singular configuration. For the optimization runs of the redundant 3-PRRR manipulator, limits were placed on the displacements of the base prismatic joint. The range of limits on these prismatic joint is from 0.05 m to 0.1 m. In theory, when the position of the actuated joints changes simultaneously the constant-orientation workspace and singularity points are also changes, this range is selected in a way that for all the positions of the prismatic joint the singularity points are falls under the same region where the trajectory is considered as shown in Fig.2.

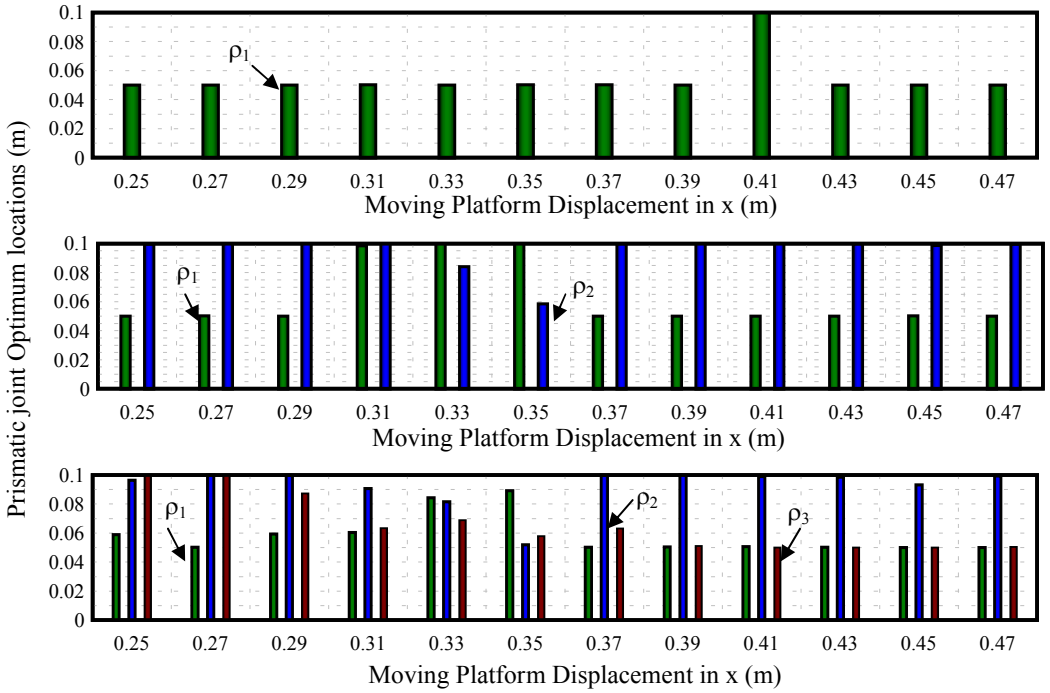


Fig. 4 Prismatic joints optimum points at minimum torques

Fig.4 shows the prismatic joint optimum locations of 1-DOKR, 2-DOKR and 3-DOKR redundant 3-PRRR manipulator respectively where the joint torques are minimum in each time step for the straight line trajectory. And Fig.5 shows the optimized torques for the redundant 3-PRRR manipulator for 1-DOKR and it clearly shows that the joint torques of the redundant manipulator are lower than the non-redundant manipulator. This demonstrates that the actuated torques is being optimized. Comparing Fig.3 with Fig.5, it can be seen that the redundant manipulator easily passes through the singular configuration, while maintaining feasible actuated joint torques. This ability to avoid singular configurations is one of the main advantages of using a redundant manipulator compared to a non-redundant manipulator. Similarly results are showed for 2-DOKR and 3-DOKR in Fig.6. When increasing the degrees of redundancy the actuated joint torques are much minimizing.

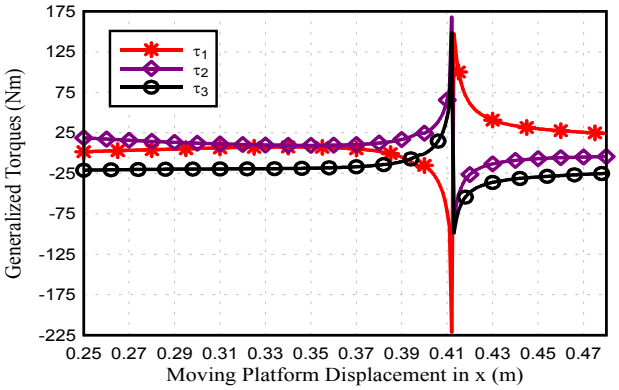


Fig. 5 Actuator optimized torques for the 3-PRRR manipulator for the straight-line trajectory

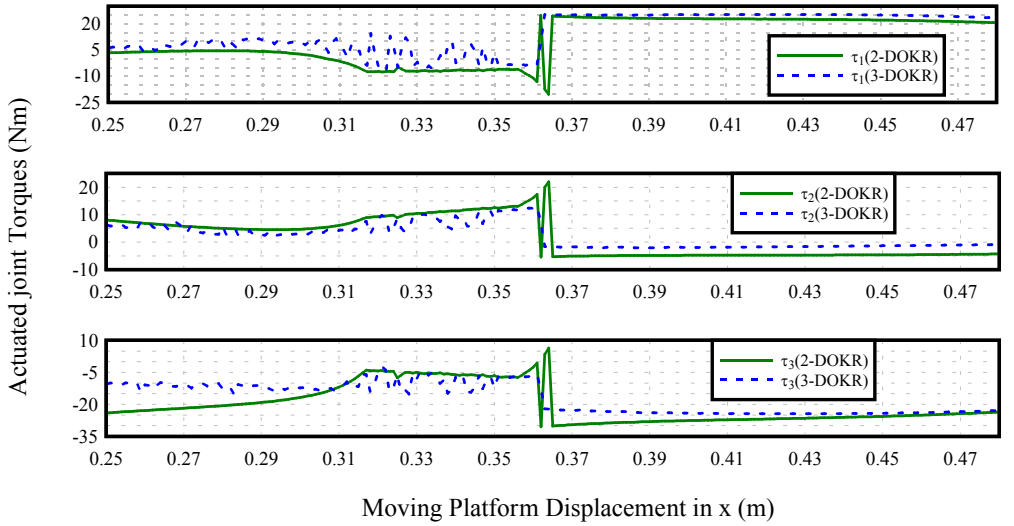


Fig. 6 Actuator optimized torques for the 3-PRRR manipulator for the straight-line trajectory

## 6. Conclusions

In present formulation, optimized redundant prismatic joint locations of planar 3-PRRR parallel mechanism for obtaining minimum joint torques were obtained. The methodology was illustrated using the system following a straight line trajectory of end-effector. The results indicate that the kinematically-redundant manipulator has improved performance over the non-redundant device. The optimized torques required by the actuators of the redundant manipulator was much lower than those of the non-redundant manipulator. To avoid the complexity of selecting the bounds on prismatic joint variables, the formulation can be extended with dexterity constraints also.

## References

[1] Kock S, Schumacher W. A parallel x-y manipulator with actuation redundancy for high-speed and active-stiffness applications. Proc. of the IEEE Int Conf on Robotics and Automation 1998; 2295–2300.
[2] Muller A. Internal preload control of redundantly actuated parallel manipulators & its application to backlash avoiding control. IEEE Transactions on Robotics and Automation 2005; 21(4): 668–677.
[3] Ebrahimi I, Carretero JA, Boudreau R. Path Planning for the 3-PRRR Redundant Planar Parallel Manipulator. Proc. of the IFToMM World Congress, Besanc on, France; 2007.
[4] Ebrahimi I, Carretero JA, Boudreau R. Kinematic Analysis and Path Planning of a New Kinematically Redundant Planar Parallel Manipulator. J of Robotica 2008; 26(3): 405–413.
[5] Wang J, Gosselin CM. Kinematic Analysis and Design of Kinematically Redundant Parallel Mechanisms ASME J Mech Des 2004; 126(1): 109–118.
[6] Ebrahimi I, Carretero JA, Boudreau R. 3-PRRR redundant planar parallel manipulator: inverse displacement, workspace and singularity analyses. J Mech and Mach Theory 2007; 42 (8):1007–1016.
[7] Ebrahimi I, Carretero JA, Boudreau R. A Family of Kinematically Redundant Planar Parallel Manipulators J Mech Des 2008; 130: 0623061-8
[8] Cha SH, Lasky TA, Velinsky SA. Kinematically-redundant variations of the 3-RRR mechanism and local optimization-based singularity avoidance. J Mechanics Based Design of Structures and Machines 2007; 35(1): 15–38.
[9] Cha SH, Lasky TA, Velinsky SA. Determination of the kinematically redundant active prismatic joint variable ranges of a planar parallel mechanism for singularity-free trajectories, J Mech and Mach Theory 2009; 44 (5):1032–1044.
[10] Weihmann L, Martins D, Coelho LS. Force capabilities of kinematically redundant planar parallel manipulators. Proc. of the 13th World Congress in Mechanism and Machine Science; 2011.
[11] Boudreau R, Nokleby S. Force optimization of kinematically-redundant planar parallel manipulators following a desired trajectory. J Mech and Mach. Theory 2012; 56: 138–155.
[12] Firmani F, Podhorodeski RP. Singularity Analysis of Planar Parallel Manipulators based on Forward Kinematic Solutions. J Mech Mach Theory 2009; 44: 1386-1399.
[13] Goldberg, D. E. (1989). Genetic Algorithms in Search, Optimization and Machine Learning. Addison-Wesley, Reading, Massachusetts.